Thin-film photosensor design for liquid crystal spatial light modulators

Pierre R. Barbier*
Li Wang
Garret Moddel
University of Colorado
Electrical and Computer Engineering
Department and Optoelectronic
Computing Systems Center
Boulder, Colorado 80309-0425
E-mail: moddel@boulder.colorado.edu

Abstract. Liquid crystal (LC) spatial light modulators (SLMs) are addressed optically with semiconductor thin-film photosensors incorporated into the devices. Nematic LCs, which are insensitive to the polarity of the applied voltage, are addressed by optically modifying the effective resistance of the photosensors to be much smaller than or much larger than a threshold value. Much faster ferroelectric LCs, which are polarity sensitive, are addressed by supplying sufficient photogenerated charge. Because the spatial resolution of the devices decreases rapidly with increasing mobility of carriers at the photosensor/LC interface, very low mobilities, less than 1 $cm^2\ V^{-1}\ s^{-1}$, are required. Photodiodes of hydrogenated amorphous silicon in *p-i-n,* Schottky, and metal insulator semiconductor configurations form practical photosensors for optically addressed SLMs. Thin-film photoconductors, having nonblocking contacts, cannot be used in many cases because of their large dark currents.

Subject terms: photosensors; photodiodes; photoconductors; hydrogenated amorphous silicon; spatial light modulators; liquid crystals; ferroelectric liquid crystals; nematic liquid crystals.

Optical Engineering 33(4), 1322–1329 (April 1994).

1 Introduction

Optically addressed spatial light modulators (OASLMs) are devices that alter the properties of a readout light beam in response to an input write image. They are key elements of optical processing. They can perform wavelength conversion, coherent-to-incoherent image conversion, and intensity amplification of 2-D images. OASLMs are formed from a sandwich of a photosensor layer, which absorbs a write-light image to create a spatially varying electric field, and a modulating layer, which responds to the electric field to modulate a read light that passes through it.

High-performance OASLMs have been fabricated by assembling light-modulating liquid crystals (LCs) with thin-film photosensors.[1] Critical parameters in OASLM photosensors are photosensor thickness, high lateral resistivity, and good photoresponse. Although LC OASLMs are 2-D imaging devices, they may not include patterned pixels. In this case their spatial resolution depends only on the LC and photosensor material properties and may be high compared to patterned devices. In this paper we review thin-film photosensors that have been incorporated into LC OASLMs. We discuss the optoelectronic and physical properties that the photosensor must fulfill in such OASLMs and present experimental characteristics of different types of hydrogenated amorphous silicon photosensors.

*Current affiliation: Laboratory for Physical Sciences, 8050 Greenmead Drive, College Park, MD 20740.

Paper 10083 received Aug. 19, 1993; accepted for publication Oct. 25, 1993.

2 Liquid Crystals

An LC is a birefringent medium whose optical axes can rotate under the influence of an externally applied electric field, modifying the polarization of a light beam that passes through it. By an appropriate orientation of polarizers and crossed analyzers, this polarization change may be transformed into an intensity modulation. Two types of LCs have been commonly incorporated into OASLMs: nematic liquid crystals (NLCs) and ferroelectric liquid crystals (FLCs).[2] Both types of LCs can be inserted between two transparent electrodes whose surfaces have been previously coated with an alignment layer to orient the LC molecules. The resulting LC cells are driven by applying a voltage waveform across the two transparent electrodes. Although they both produce a rotation of the polarization of transmitted light, NLC and FLC cells respond differently to an applied voltage, and thus require different photosensor configurations.

NLCs respond to the magnitude of the external electric field independent of its polarity. As a consequence, NLCs are usually driven with dc-balanced voltage waveforms such as sine waves. Several types of NLC cell structures have been used to make OASLMs. In the birefringent mode, the NLC molecules are parallel to each other and to the substrates in the absence of an applied voltage.[3] When a sufficiently large voltage is applied to the cell, the molecules rotate perpendicularly to the substrates. The transfer characteristic of a birefringent-mode NLC cell is illustrated in Fig. 1 where the optical response is plotted versus the rms value of the applied voltage. Other NLC alignment modes that have been used in OASLMs are the twisted nematic mode and the hybrid field mode, discussed elsewhere.[4]

The thickness of NLC cells is typically 5 to 10 μm. NLC cells are driven with 1- to 10-kHz voltage sine waves whose amplitudes are ~5 V. The switching-on time of NLC cells is ~100 μs, but their switching-off time is much longer, ~20 ms. To switch the NLC cell of Fig. 1 on and off and to optimize the contrast ratio, the rms value of the sine-wave applied voltage must equal $\langle V_{on} \rangle$ and $\langle V_{off} \rangle$, respectively.[5]

FLCs respond to the polarity and magnitude of an externally applied electric field. By an appropriate choice of the alignment layers, FLC cells can be made bistable such that the orientation is maintained when the applied voltage is switched to zero.[6] The transfer characteristic of a bistable FLC cell is illustrated in Fig. 2, where its optical transmission between crossed polarizers is plotted versus applied voltage.

The thickness of FLC cells is typically 1 to 2 μm. FLCs switch much more quickly than NLCs. Their switching time is inversely proportional to the applied voltage and is ~50 μs when 10 V are applied to a 1-μm-thick FLC cell. Because they require fields of both polarities to switch on and off, FLC cells are driven with voltage pulses or square waves. In the remainder of this paper, an FLC cell will be assumed to switch on in response to a negative and off to a positive applied voltage, as represented in Fig. 2.

3 Optically Addressed Spatial Light Modulators

The cross section of a general LC OASLM is shown in Fig. 3. The LC is sandwiched between a transparent conducting oxide (TCO) electrode that has been deposited onto a glass plate and a photosensor. The photosensor may be a deposited thin-film semiconductor or a crystalline semiconductor wafer. A dielectric stack reflector may be deposited on top of the photosensor to enhance reflection of the readout light. Prior to assembly, the two LC-bounding surfaces must be coated with alignment layers. To achieve uniform LC thickness and avoid wavefront distortion of the readout beam, optical flats are used and smooth photosensors are fabricated.

LC OASLMs are driven with voltage waveforms applied to the two TCO electrodes. In the absence of illumination only a small fraction of the applied voltage drops across the LC, which remains in what is defined as the *off state*. When and where a write image is incident onto the photosensor, a photocurrent flows and a larger fraction of the applied voltage drops across the LC, which switches to its *on state*. A uniform linearly polarized readout beam is incident onto the LC side of the OASLM and is reflected by the dielectric stack reflector—or by the photosensor/LC interface if there is no reflector. The readout light passes through the LC twice and its polarization is rotated where and when the LC molecules have switched. The polarization rotation may then be transformed into an intensity modulation after filtering through a crossed polarizer. In summary, an LC OASLM can form an intensity replica of an incident write image.

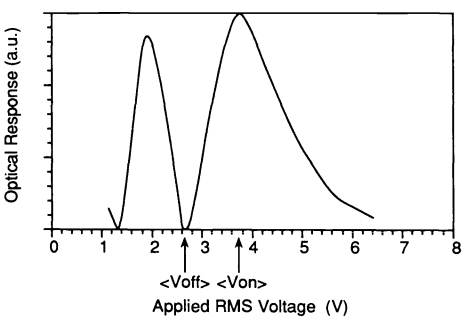

Fig. 1 Transfer characteristic of a 4-μm-thick NLC cell in the parallel-alignment birefringent mode driven with a 5-kHz sine wave.

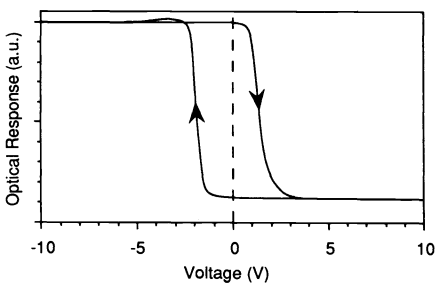

Fig. 2 Transfer characteristic of a 2-μm-thick FLC cell.

4 Photosensor

The role of the photosensor is to transfer the OASLM driving voltage to the LC when and where the photosensor is illuminated with a write light. Since NLCs are driven with dc-balanced voltage sine waves, the photosensor of an NLC OASLM should ideally have a symmetric current-voltage characteristic such as that of a photoconductor. In fact, this requirement is loose because of the dielectric stack reflector that is often incorporated into an NLC OASLM to increase the reflected readout light intensity. The effect of such a dielectric stack is to introduce a series capacitance into the OASLM that absorbs any asymmetry in the time-averaged voltage waveforms across the LC.[7] As a consequence, the voltage across the NLC is dc-balanced even though the photosensor may have an asymmetric current-voltage characteristic, e.g., that of a photodiode. The role of the photosensor in an NLC OASLM is to modulate the rms value of the voltage across the LC between $\langle V_{off} \rangle$ and $\langle V_{on} \rangle$ represented in Fig. 1, when the write light is off and on, respectively. The design of an NLC OASLM is then an impedence matching problem as addressed in Sec. 4.1.1.

As FLCs respond to the sign of the applied voltage, the photosensor and/or the driving waveform of an FLC OASLM must provide an asymmetric current-voltage characteristic. An FLC OASLM is generally operated with a voltage square wave. The role of the photosensor in an FLC OASLM is to provide sufficient charge to switch off the FLC during the positive period of the OASLM driving voltage waveform, and to keep the FLC off during the subsequent negative period

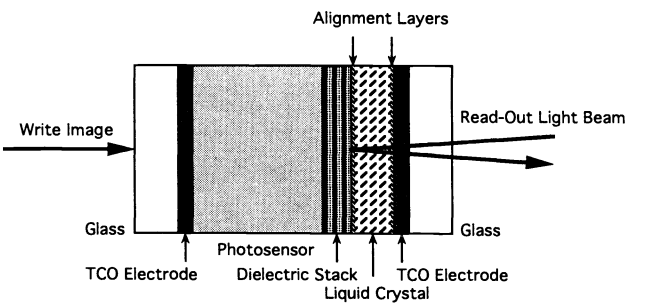

Fig. 3 Cross section of an LC OASLM incorporating a dielectric stack reflector.

in the absence of write light. Additionally, the photosensor must provide sufficient charge to switch the FLC on during the negative voltage period in the presence of a write light. (This description is based on the FLC on and off states defined in Fig. 2, where the applied voltage is negative or positive, respectively.) The design of an FLC OASLM is also a capacitance matching problem, since each time there is a voltage applied to the OASLM there is a corresponding voltage step across the FLC that may cause the unintentional switching on of the FLC in the absence of write light. The photosensor electrical requirements for FLC OASLMs are discussed in Sec. 4.1.2.

4.1 *Electrical Requirements*

In this section we discuss the electrical requirements that photosensors must fulfill to operate successfully in NLC and FLC OASLMs. These requirements are derived from a simple analysis of the OASLM equivalent circuits.[8,9] Since NLC and FLC OASLMs are driven differently, their photosensors must satisfy different requirements.

4.1.1 *Nematic liquid crystal optically addressed spatial light modulators*

We consider an OASLM incorporating a dielectric stack reflector, the NLC whose transfer characteristic is shown in Fig. 1, and a photosensor exhibiting symmetric current-voltage characteristics (photoconductor). In the absence of write light the rms value of the voltage waveform across the NLC must equal $\langle V_{\text{off}} \rangle$ in Fig. 1.[10] For the purposes of this analysis we model the OASLM with the simple equivalent circuit shown in Fig. 4. Thus,

$$\frac{\langle V_{\text{off}} \rangle}{\langle V_{\text{app}} \rangle} = \frac{C_{\text{PS}} C_{\text{DS}}}{C_{\text{PS}} C_{\text{DS}} + C_{\text{DS}} C_{\text{LC}} + C_{\text{LC}} C_{\text{PS}}} , \tag{1}$$

where C_{LC}, C_{DS}, and C_{PS} are the capacitances of the (unswitched) liquid crystal, the dielectric stack reflector, and the photosensor, respectively, and $\langle V_{\text{app}} \rangle$ is the rms value of the applied-voltage sine wave. (This relation can be simplified for an OASLM without a dielectric stack by setting $C_{\text{DS}} = +\infty$.)

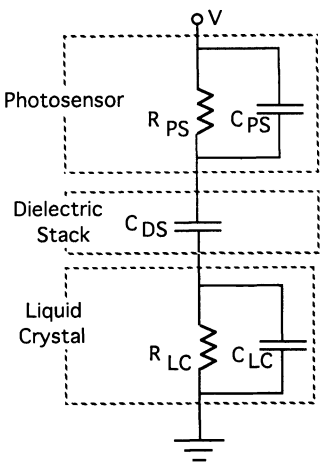

Fig. 4 Simple equivalent circuit for an OASLM in which the photosensor is modeled as a photoconductor.

To switch the NLC on in the presence of a write light, with the assumption that no voltage drops across the photosensor, the rms voltage across the LC must equal $\langle V_{\text{on}} \rangle$ in Fig. 1, yielding

$$\frac{\langle V_{\text{on}} \rangle}{\langle V_{\text{app}} \rangle} = \frac{C_{\text{DS}}}{C_{\text{DS}} + C_{\text{LC}}} . \tag{2}$$

Knowing C_{DS}, C_{LC}, $\langle V_{\text{off}} \rangle$, and $\langle V_{\text{on}} \rangle$, the design and operation of an NLC OASLM may be developed from Eqs. (1) and (2), which have two unknowns, C_{PS} and $\langle V_{\text{app}} \rangle$. Quantitatively, taking $\langle V_{\text{off}} \rangle = 2.2$ V and $\langle V_{\text{on}} \rangle = 2.7$ V from Fig. 1, and assuming $C_{\text{LC}} = 1$ nF/cm^2 and $C_{\text{DS}} = 10$ nF/cm^2, the solution of Eq. (1) and Eq. (2) is $\langle V_{\text{app}} \rangle = 4.1$ V and $C_{\text{PS}} = 2.4$ nF/cm^2. This capacitance corresponds to an ~4-μm-thick hydrogenated amorphous silicon (a-Si:H) film (using $C_{\text{PS}} = \varepsilon_{\text{PS}} / d_{\text{PS}}$ where ε_{PS} and d_{PS} are the dielectric constant and the thickness of the photosensor, respectively).[10]

Additional conditions to insure proper operation of NLC OASLM are that the photosensor dark resistance R_{PS}(dark) be sufficiently large that the rms value of the voltage across the NLC equals $\langle V_{\text{off}} \rangle$ and that the photosensor resistance R_{PS}(light) in the presence of a write light is sufficiently small that the voltage across the NLC is equal to $\langle V_{\text{on}} \rangle$. This is a resistance-capacitance (RC) time constant requirement in which the OASLM RC time constant is assumed to be larger or smaller than the OASLM driving frequency f in the dark or in the light, respectively. This is the case if

$$R_{\text{PS}}(\text{dark}) \gg R_{th} \gg R_{\text{PS}}(\text{light}) ,$$

where

$$R_{th} = \frac{1}{2\pi f \left[C_{\text{PS}} + \dfrac{C_{\text{LC}} C_{\text{DS}}}{C_{\text{LC}} + C_{\text{PS}}} \right]} . \tag{3}$$

Using the previous values and $f = 5$ kHz, Eq. (3) yields $R_{th} = 10$ kΩ cm^2. This resistance is so high, corresponding to a bulk conductivity of 4×10^{-8} Ω^{-1} cm^{-1} for a 4-μm-thick photosensor, that one generally makes use of a barrier rather than bulk resistivity to attain the desired effective dark resistance.

This discussion applies to an NLC OASLM incorporating a photoconductor and not a photodiode. In the photodiode case a similar analysis can be performed by distinguishing the voltage drive periods during which the photodiode is reverse and forward biased.[7]

4.1.2 *Ferroelectric liquid crystal optically addressed spatial light modulators*

Since FLCs respond to the magnitude and sign of the applied voltage, FLC OASLMs are operated typically with voltage square waves.[2] We consider an FLC OASLM that is driven with a V_- (<0) to V_+ (>0) voltage square wave of frequency f. In the absence of a write light, the dark current of the photosensor during the negative-voltage cycles of the OASLM must be sufficiently small so that it does not charge the FLC capacitance and switch on the FLC. Thus, the negative-voltage dark current I_d must be smaller than

$$I_d \ll 2f(C_{LC}+C_{PS})|V_-| \ , \tag{4}$$

where C_{LC} and C_{PS} are the LC and the photosensor capacitances, respectively. Another requirement to prevent undesired switching on of the FLC in the absence of write light is that the voltage across the FLC resulting from the capacitance bridge divider is not negative after each negative-voltage step of the OASLM driving voltage square wave. Assuming that the voltage square wave is dc balanced to optimize the sensitivity of the OASLM,[8] this requirement implies that

$$C_{PS}=C_{LC} \ , \tag{5}$$

which is equivalent to

$$\frac{d_{PS}}{\varepsilon_{PS}}=\frac{d_{LC}}{\varepsilon_{LC}} \ , \tag{6}$$

where d_{PS} and ε_{PS} are the thickness and the dielectric constant of the photosensor, respectively, and d_{LC} and ε_{LC} are the thickness and the dielectric constant of the liquid crystal, respectively.

To fully switch off (erase) the FLC, the photosensor must supply sufficient charge during the positive applied-voltage period. This charge may be supplied by a forward-biased photodiode or by a photoconductor uniformly illuminated with a flushing beam. In both cases, the minimum current I_{erase} necessary to erase the FLC must be much larger than

$$I_{erase} \gg 2f[(C_{LC}+C_{PS})|V_+|+2P] \ , \tag{7}$$

where P is the spontaneous polarization of the FLC.

Quantitatively, the thickness and thus the capacitance of the FLC is determined by the FLC birefringence optical quarter-wave condition at the readout light wavelength; typically, $d_{LC}=1$ μm (at 632.8 nm) and $C_{LC}=5$ nF/cm^2. Thus, Eqs. (5) and (6) yield $C_{PS}=5$ nF/cm^2 and $d_{PS}=3$ μm, respectively. If the OASLM is operated with a 1-kHz, −10- to +10-V square wave and $P=25$ nC/cm^2, Eqs. (4) and (7) yield $I_d \ll 200$ μA/cm^2 and $I_{erase} \gg 300$ μA/cm^2, respectively. The achievable values of $I_d=10$ μA/cm^{2}and $I_{erase}=1$ mA/cm^2 are sufficient.

4.2 *Photosensor Collection Efficiency and OASLM Sensitivity*

As mentioned earlier, the NLC of an NLC OASLM is switched on and off by varying RC time constants within the OASLM. Thus, the write-light sensitivity of an NLC OASLM is related to the minimum write-light intensity that is necessary to decrease the LC-associated RC time constant sufficiently, and hence to decrease the photosensor resistance to less than the threshold value R_{th} given in Eq. (3). Expressing the photosensor resistance in terms of light intensity, collection efficiency, carrier lifetime, and photon energy, the minimum write-light intensity to switch on an NLC OASLM can be derived simply and is equal to

$$P_{min}=\frac{d_{PS}^2 h\nu}{q\mu R_{th}\eta\tau} \ , \tag{8}$$

where d_{PS} is the photosensor thickness, $h\nu$ is the photon energy, q is the elementary electronic charge, μ is the majority carrier drift mobility, η is the collection efficiency, and τ is the carrier lifetime. If the photosensor is a photodiode then the carrier lifetime is approximately equal to $1/2f$. Using the previous values for a thin-film photosensor of $\mu=1$ cm^2 V^{-1} s^{-1}, $\eta=1$, $\tau=100$ μs, and $h\nu=2$ eV, the theoretical minimum write-light intensity to switch on an NLC OASLM is 0.5 μW/cm^2, and 100 μW/cm^2 experimentally. Presumably the large difference between the theoretical and experimental values is that the experimental τ is much shorter than the NLC response time. The minimum intensity can be reduced by increasing the carrier lifetime in the photosensor. However, if the carrier lifetime is longer than the NLC relaxation time, it limits the OASLM response time.

The switching of the FLC in an FLC OASLM is controlled by the charge that is provided by the photosensor to the FLC instead of by the phototransport parameters of Eq. (8) that limit NLC OASLM sensitivity. The minimum charge that must be supplied by the photosensor to switch on the FLC is approximately equal to $2P$, where P is the spontaneous polarization of the FLC. The sensitivity of an FLC OASLM is related to the minimum write-light energy that is necessary for the photosensor to provide a charge of $2P$. This minimum energy is equal to

$$Q_{min}=\frac{2Ph\nu}{\eta q} \ , \tag{9}$$

where $h\nu$ is the photon energy and η is the photosensor collection efficiency. For $P=25$ nC/cm^2, $h\nu=2.0$ eV, and $\eta=1$, the minimum write-light energy to switch on an FLC OASLM fully is 100 nJ/cm^2. For a square-wave driving frequency of 1 kHz, this corresponds to a write-light intensity of 200 μW/cm^2. In this case the theoretical and experimental values agree.

For both types of OASLMs it is desirable to improve the sensitivity and thus to have a photosensor collection efficiency that is as large as possible. A photodiode can have a maximum collection efficiency of only $\eta=1$ in reverse bias. A photosensor with gain would be better but cannot be easily fabricated and incorporated in LC OASLMs.

4.3 *Photoresponse Time*

In most cases the OASLM switching time is limited by the LC switching, which is usually slower than the photosensor photoresponse. As mentioned previously, NLC and FLC switching times are ~20 ms and ~50 μs, respectively. However, if the photoresponse of the photosensor is slower than the LC switching, a residual image (also called image lag) may appear in the OASLM. This is the case with photosensor materials that have a large density of deep states[11] such as CdS. To avoid this problem it is desirable to use materials that have a fast response,[12] such as crystalline Si or a-Si:H.

4.4 *Resolution*

The spatial resolution is a critical parameter in OASLM performance. It is defined by the number of distinguishable dark and bright line pairs per unit length and is usually expressed in line pairs per millimeter (lp/mm). In a pixelated OASLM the resolution depends on the size and pitch of the pixels. In a uniform photosensor OASLM the resolution is determined by the photosensor electronic transport properties and thick-

ness and varies inversely with the thicknesses of the photosensor and the LC. FLC OASLM resolution has been measured experimentally up to 110 lp/mm (at 50% modulation transfer function) with an a-Si:H photosensor that is ~2 μm thick.[13] Several models have been proposed to understand OASLM resolution limitations. However, these models ignore time-dependent lateral carrier spreading and do not apply to LC OASLMs.[14–16] We present in this paper the basis for a new model in which we consider this charge spreading.

In this model we consider the spreading of the electrons at the photosensor/LC interface. At this interface we assume a sinusoidal electron photogeneration rate resulting from the write-light fringe pattern. The electron generation rate distribution per unit area is

$$g(x,t)=\begin{cases}0 & \text{for } t\leq 0\\ g_0[1+m\cos(\nu x)] & \text{for } t>0\end{cases}, \tag{10}$$

where $\nu=2\pi f_x$ and f_x is the spatial frequency of the write-light fringes, and g_0 and m are the carrier generation rate mean intensity and fringe visibility, respectively.

The 1-D current continuity equation is

$$\frac{\partial\sigma(x,t)}{\partial t}=\frac{1}{q}\frac{\partial J(x,t)}{\partial x}+g(x,t)\ , \tag{11}$$

where $\sigma(x,t)$ is the surface carrier density and $J(x,t)$ is the lateral current density. The lateral current due to diffusion and drift is equal to

$$J(x,t)=qD\frac{\partial\sigma(x,t)}{\partial x}+q\mu\sigma(x,t)E_x(x,t)\ , \tag{12}$$

where D is the electron diffusion coefficient that is equal to $kT\mu/q$ using the Einstein relationship, kT is the thermal energy, μ is the electron mobility, and $E_x(x,t)$ is the lateral electric field at the LC/photosensor interface.

The solution of Eqs. (11) and (12) cannot be derived analytically and must be solved numerically.[17] However, neglecting the drift current, i.e., setting $E_x(x,t)=0$, the analytical solution of Eqs. (11) and (12) using the initial condition of Eq. (10) is

$$\sigma(x,t\geq 0)=\sigma(x,0)+g_0t\left[1+m\frac{1-\exp(-D\nu^2t)}{D\nu^2t}\cos(\nu x)\right]. \tag{13}$$

This charge distribution at the photosensor/LC interface yields a voltage profile across the LC. The LC switches on and off as a function of this voltage profile. To find the resolution of an OASLM, the modulation transfer function (MTF), which is defined as the ratio of the visibilities of the output optical response to that of the input write-light intensity fringe pattern, is measured. Since the exact optical response of the LC cannot be calculated as a simple function of the voltage and of the time, we give the MTF of the voltage profile in response to the write light. This voltage profile can be derived from Eq. (13) and Poisson's equation. The result is

$$\mathrm{MTF}(t\geq 0)=\frac{\dfrac{\varepsilon_{LC}}{d_{LC}}+\dfrac{\varepsilon_{PS}}{d_{PS}}}{[\varepsilon_{LC}\coth(\nu d_{LC})+\varepsilon_{PS}\coth(\nu d_{PS})]\nu}\,\frac{q\left[1-\exp\left(\dfrac{-kT\mu\nu^2t}{q}\right)\right]}{kT\mu\nu^2t}\ . \tag{14}$$

The first term of Eq. (14) corresponds to the thickness-limited resolution and the second term to the carrier-diffusion-limited resolution.

The voltage MTF at $t=0.5$ ms, corresponding to the end of an FLC OASLM write cycle at 1 kHz, is plotted in Fig. 5 as a function of the spatial frequency. We also plotted in the figure the numerically solved MTF resulting from both diffusion and drift of the electrons at the LC/photosensor interface (curve d′).

As Fig. 5 shows, the MTF increases with decreasing photosensor thickness, in agreement with previous models.[14,16] The MTF decreases with increasing carrier mobility, confirming the experimental results that low-mobility photosensors yield higher resolution OASLMs than high-mobility photosensors.[2] From this simulation it appears that a very low mobility is desirable, but in fact the trapping of the carriers by the semiconductor surface states or carrier localization by the LC might improve the resolution even if higher mobility photosensors are used. An OASLM incorporating a photosensor with an extremely low carrier mobility may exhibit poor response time and sensitivity. We will present a more detailed model in a future publication.[17]

4.5 *Physical Requirements*

Photosensors for OASLMs must be compatible with LC technology. Two classes of photosensor materials have been used. Wafers of crystalline semiconductors[5,18,19] such as Si, GaAs, and BSO have been used directly or bonded onto TCO-coated optical flats and polished to make OASLMs. However, crystalline semiconductor wafers are thick and have a high carrier mobility, and thus yield low spatial resolution OASLMs. To improve OASLM resolution, some crystalline wafer photosensors have been thinned and/or patterned with an array of photodiodes or etched pixels. These processing steps add

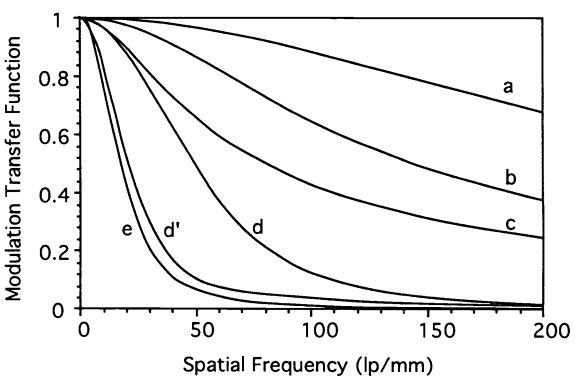

Fig. 5 Theoretical voltage MTF of an OASLM at various photosensor thicknesses and carrier mobilities using $d_{LC}=1$ μm, $\varepsilon_{LC}=4\,\varepsilon_0$, and $\varepsilon_{PS}=12\,\varepsilon_0$, where ε_0 is the permittivity of vacuum. These curves were calculated neglecting carrier drift [Eq. (14)] as follows. a: $d_{PS}=1$ μm, $\mu=0$; b: $d_{PS}=3$ μm, $\mu=0$; c: $d_{PS}=10$ μm, $\mu=0$; d: $d_{PS}=3$ μm, $\mu=0.01$ cm^2 V^{-1} s^{-1}; and e: $d_{PS}=3$ μm, $\mu=0.1$ cm^2 V^{-1} s^{-1}. Curve *d′* was obtained as in curve *d* but including the effect of carrier drift at the LC/photosensor interface.

fabrication complexity and cost to the OASLM. Consequently, it is preferable to use deposited thin films that have a low carrier mobility. Thin-film semiconductors[2,10,11,20] such as CdS and a-Si:H have been deposited directly onto TCO-coated optical flats to make OASLMs. However, CdS has a long photoresponse time that limits OASLM frame rates. Unlike CdS, a-Si:H has a much faster photoresponse time and is becoming the photosensor of choice for both NLC and FLC OASLMs. Because of capacitance matching, NLC OASLMs require thicker photosensors than do FLC OASLMs. For this reason, thick crystalline-wafer photosensors as well as thick deposited films may be incorporated into NLC OASLMs. On the other hand, FLC OASLMs incorporate thinner photosensors that cannot be easily obtained from crystalline wafers. Thus, deposited thin films are better for FLC OASLMs.

To obtain optically uniform devices, the LC thickness must be constant over the whole OASLM area. The photosensor must be in contact with an electrode that is transparent to the write light. The opposing substrate must be transparent to the readout light and provide an electrode. For these reasons, TCO-coated $\lambda/10$ optical flats are used to fabricate OASLMs. Similarly, the photosensor surface must be smooth over the entire OASLM area. Thickness uniformity can be achieved by an appropriate choice of the geometry of the substrate and substrate holder in an a-Si:H plasma-enhanced chemical-vapor-deposition system.

Following deposition of a thin film, two types of physical defects in the thin-film photosensor may impede proper fabrication and operation of an LC OASLM. Pinholes in the photosensor thin film result in a region of the LC that cannot be write-light modulated in an OASLM. Bumps, consisting of protrusions of photosensor material, may short the two TCO electrodes or prevent the LC from being adequately thick. These defects may be prevented by using a careful cleaning procedure for the substrates before the deposition of a-Si:H.

5 Photosensor Current-Voltage Characteristics

In this section we present experimental results for four types of a-Si:H photosensors, three of which are commonly incorporated into FLC OASLMs. These are the *p-i-n* photodiode, the indium tin oxide (ITO)/a-Si:H photoconductive diode, the ITO/SiO_x/a-Si:H metal-insulator-semiconductor (MIS) photodiode, and the *n-i-n* photoconductor. Their thickness is approximately 2.5 μm to match the FLC capacitance [Eq. (5)]. The transition from photoconductors through photoconductive diodes to photodiodes is gradual and depends on the degree to which the contacts are blocking.

The current-voltage characteristics of an ~2.5-μm-thick a-Si:H *p-i-n* photodiode are shown in Fig. 6. As is apparent from the figure, this photodiode exhibits excellent rectifying behavior. It has a low reverse-bias dark current that does not switch on the FLC in the absence of illumination [Eq. (4)] and a large forward-bias current to switch the FLC off [Eq. (7)]. Under illumination it can also supply enough photocurrent in reverse bias to switch on the FLC.

The collection efficiency of this *p-i-n* photodiode under −5-V reverse bias is ~80% at 514.5-nm wavelength. Its photoresponse time is short, as shown in Fig. 7(a). However, because a-Si:H has a large density of deep states there is a slow component to the current decay following a forward-

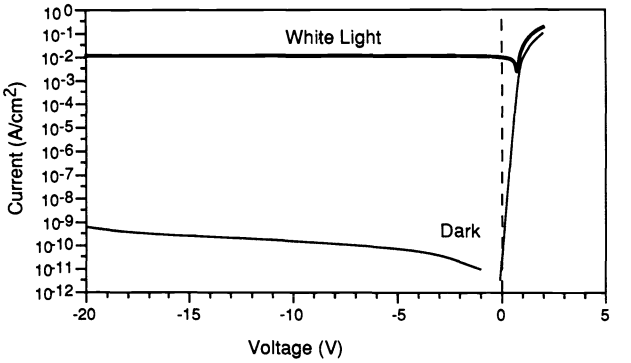

Fig. 6 Current-voltage characteristics of a 2.5-μm a-Si:H *p-i-n* photodiode in the dark and under ~50-mW/cm² white-light illumination.

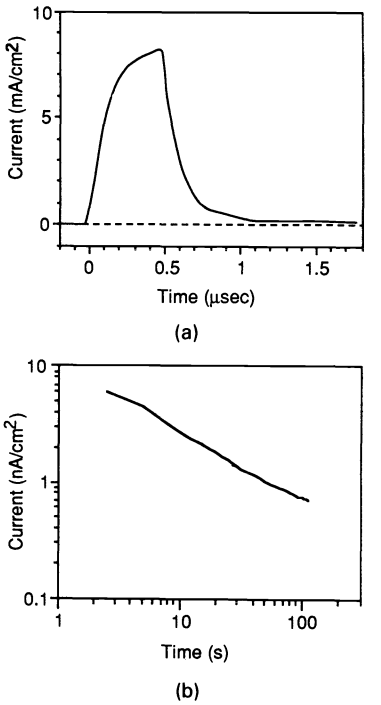

Fig. 7 Photocurrent response of a ~2.5-μm-thick *p-i-n* photodiode reverse biased at −5 V in response to (a) 50-ns light pulse (50 mW/cm² at 514.5 nm) and (b) 1-ms light pulse (1 mW/cm² at 514.5 nm).

biasing voltage step or a light pulse, as shown in Fig. 7(b). The current continues to decay until a steady state is reached when the dark current is composed of a thermal generation current.[21] This current decay may contribute to the formation of a residual image in an OASLM, in which the LC of the OASLM would switch on long after a write image was incident onto the photosensor. Experimental studies[8] have shown that there is no significant residual image effect in an OASLM incorporating an a-Si:H photosensor because the residual current is sufficiently low [note the current scale on Fig. 7(b)], which was not the case with an OASLM[11] including CdS.

A large forward-bias current is necessary to switch off the FLC in an OASLM. In a previous study we showed that in a *p-i-n* photodiode only electron injection controls the erase

of the OASLM because holes do not have time to significantly contribute to the transient current.[22] Thus, the role of the *p*-layer in the *p-i-n* photodiode of an OASLM is not to enhance hole injection under forward bias, but rather to prevent the injection of electrons from the TCO electrode in contact with the *p*-layer, which may switch on the FLC in the dark under reverse bias.

An a-Si:H photoconductive diode (PCD) operates as a somewhat leaky a-Si:H *p-i-n* photodiode in series with a photoresistance. An Mg/Ag contact was deposited on top of an ~2.5-μm-thick PCD to form a relatively nonblocking back contact.[23] The current-voltage characteristics of this PCD are shown in Fig. 8. Both the dark and illuminated characteristics are not symmetric near 0 V because the ITO and Mg/Ag contacts on a-Si:H form Schottky barrier diodes of different heights, 0.7 and 1 eV, respectively.[23,24] Note that the current-voltage characteristics are not linear, nor do they follow a power law, indicating that the PCD is not a photoconductor. The current-voltage characteristics and photoresponse of the reverse-biased PCD are effectively similar to those of a *p-i-n* photodiode. Since the forward-bias dark current is small, the PCD should be illuminated with a flushing beam to supply sufficient current to fully erase the OASLM.

An a-Si:H MIS diode was fabricated by depositing an ~2.5-μm a-Si:H layer over an ~100-nm SiO_x film that had been deposited on a ITO-coated glass substrate. A Cr electrode was evaporated to form a back contact. The steady-state current-voltage characteristics of the MIS structure are shown in Fig. 9. Since the SiO_x layer is a thick insulator the steady-state current of the MIS is small. Because the insulating layer acts largely like a capacitor, the current-voltage characteristics of an MIS photodiode are time dependent. The transient photocurrents are much larger than the currents in Fig. 9, allowing FLC OASLMs that incorporate them to function properly.

The three photosensors that have been presented each have a sufficiently small dark current [see Eq. (4)], and each can supply sufficient photocurrent (or forward-bias current) to switch the FLC on (or off) when illuminated appropriately [see Eq. (7)].

We tried to incorporate a-Si:H *n-i-n* photoconductors into FLC OASLMs, as a means to improve the OASLMs' write-light sensitivities by the use of photoconductive gain. To form photoconductors the contacts must be nonblocking and may be formed with *n*-type layers. The steady-state current-voltage characteristics of a 4.1-μm-thick a-Si:H *n-i-n* photoconductor are shown in Fig. 10 in the dark and under 1-mW/cm^2 632.8-nm illumination. Even though a photoconductive gain of ~100 was obtained at 10 V with this structure, the dark current above 2 V is larger than 10^{-5} A/cm^2, the maximum value calculated in Eq. (4). This is because electrons are injected from the *n*-type contact, resulting in a space-charge-limited current that increases as the square of the voltage.[9,25] This large dark current switched on the fabricated FLC OASLM even in the absence of a write light, and thus the device could not be optically addressed. Since the space-charge-limited current is inversely proportional to the cube of the thickness,[25] the dark current would be reduced to less than the value set by Eq. (4) if the a-Si:H *n-i-n* thickness were increased[26] above ~15 μm. This thickness is not practical since it would take too long to deposit the photosensor (~30 h in our system), the resolution would degrade, and the write light would not be absorbed uniformly across the thickness. Therefore, incorporating genuine photoconductors into FLC OASLMs is not feasible.

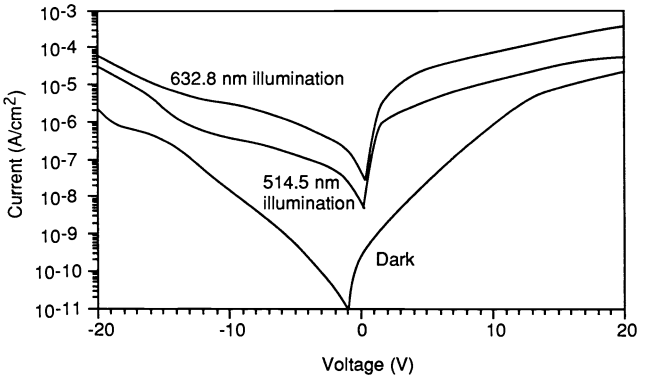

Fig. 9 Steady-state current-voltage characteristics of a 2.5-μm ITO/SiO_x/a-Si:H MIS photodiode in the dark and under 514.5-nm 400-μW/cm^2 and 632.8-nm 1.4-mW/cm^2 illumination.

6 Summary

In summary we have discussed the differences in operation of thin-film photosensors for NLC and FLC OASLMs. From the analysis of OASLM equivalent circuits we have derived design criteria such as thickness, maximum dark current, and

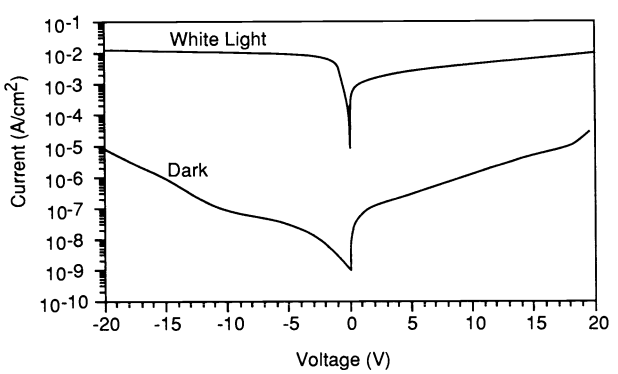

Fig. 8 Current-voltage characteristics of a 2.5-μm ITO/a-Si:H photoconductive diode in the dark and under ~50-mW/cm^2 white-light illumination.

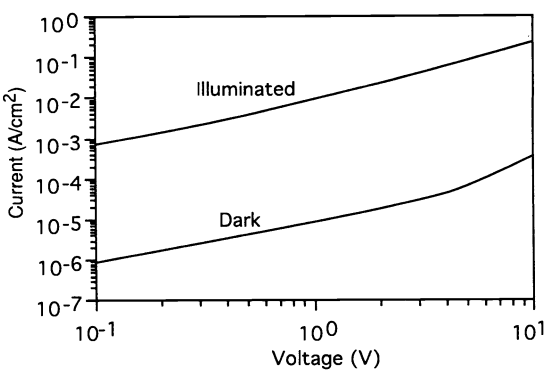

Fig. 10 Steady-state current-voltage characteristics of a 4.1-μm-thick a-Si:H *n-i-n* photoconductor in the dark and under 1-mW/cm^2 illumination at 632.8 nm.

required erase current that photosensors must fulfill to successfully drive NLC or FLC OASLMs. We have presented an improved model for the spatial resolution of LC OASLMs that accurately predicts that the resolution decreases with increasing thickness and carrier mobility in the photosensor. Finally, we showed the different experimental current-voltage characteristics of three types of a-Si:H photosensors that have been successfully included into FLC OASLMs: the *p-i-n* photodiode, the ITO/a-Si:H photoconductive diode, and the ITO/SiO_x/a-Si:H MIS photodiode. In a genuine photoconductor, having symmetric current-voltage characteristics and nonblocking *n*-type contacts, carrier injection results in a large dark current.

Acknowledgments

We thank Skip Wichart for thin-film depositions, Dave Doroski for OASLM fabrication, and Stephen Perlmutter for the experimental data of Fig. 2. This work was done under National Science Foundation Engineering Research Center Grant No. CDR-862236 and was supported by the Colorado Advanced Technology Institute.

References

1. A. D. Fisher, "Spatial light modulators: functional capabilities, applications, and devices," *Int. J. Optoelec.* **5**(2), 125–167 (1990).
2. G. Moddel, "Optically addressed spatial light modulators," Chap. 11 in *Amorphous and Microcrystalline Semiconductor Devices: Optoelectronic Devices*, J. Kanicki, Ed., Artech House, Boston (1991).
3. N. Yoshida, N. Mukohzaka, T. Hori, H. Toyoda, Y. Kobayashi, and T. Hara, "Optically addressed liquid crystal phase only modulating spatial light modulator," in *Spatial Light Modulators and Applications—Technical Digest*, Vol. 6, pp. 97–99, Optical Society of America, Washington, DC (1993).
4. J. Grinberg, A. Jacobson, W. Bleha, L. Miller, L. Fraas, D. Boswell, and G. Myer, "A new real-time non-coherent to coherent light image converter: the hybrid field effect liquid crystal light valve," *Opt. Eng.* **14**(3), 217–225 (1975).
5. K. Sayyah, M. S. Welkowsky, P. G. Reif, and N. W. Goodwin, "High performance single crystal light valve with good image uniformity," *Appl. Opt.* **28**(22), 4748–4756 (1989).
6. N. A. Clark and S. T. Lagerwall, "Submicrosecond bistable electro-optic switching in liquid crystals," *Appl. Phys. Lett.* **36,** 899–901 (1980).
7. C. Gaeta, "Analytical electrical model for a Si liquid crystal light valve," *Appl. Opt.* **30**(13), 1665–1672 (1991).
8. P. R. Barbier and G. Moddel, "Hydrogenated amorphous silicon photodiodes for optical addressing of spatial light modulators," *Appl. Opt.* **31**(20), 3898–3907 (1992).
9. P. R. Barbier, "Hydrogenated amorphous silicon photodetectors for optically addressed spatial light modulators," PhD Thesis, University of Colorado, Boulder (1993).
10. P. R. Ashley and J. H. Davis, "Amorphous silicon photoconductor in a liquid crystal spatial light modulator," *Appl. Opt.* **26**(2), 241–246 (1987).
11. C. S. Sexton, "Current status of Hughes liquid crystal light valve performance for optical data processing," in *Liquid Crystals and Spatial Light Modulator Materials, Proc. SPIE* **684,** 96–100 (1986).
12. R. D. Sterling, R. D. T. Kolste, J. M. Haggerty, T. C. Borah, and W. P. Bleha, "Video-rate liquid-crystal light-valve using an amorphous silicon photoconductor," in *SID Int. Symp., Digest of Technical Papers,* **21,** 327–329 (1990).
13. S. Fukushima, T. Kurokawa, and M. Ohno, "Real-time hologram construction and reconstruction using a high resolution spatial light modulator," *Appl. Phys. Lett.* **58**(8), 787–789 (1991).
14. D. D. Nolte, "Resolution of electro-optic spatial light modulators: the role of the lateral transport," *Opt. Comm.* **92,** 199–204 (1992).
15. Y. Owechko and A. R. Tanguay, "Theoretical resolution limitations of electrooptic spatial light modulators. I. Fundamental limitations," *J. Opt. Soc. Am. A* **1**(6), 635–643 (1984).
16. W. R. Roach, "Resolution of electrooptic light valves," *IEEE Trans. Electron. Devices* **21**(8), 453–459 (1974).
17. L. Wang and G. Moddel, University of Colorado at Boulder, Private Communication (1994).
18. M. C. Hebron and S. S. Makh, "Development of gallium arsenide-based spatial light modulators," in *Spatial Light Modulators and Applications II, Proc. SPIE* **825,** 19–23 (1987).
19. P. Aubourg, J. P. Huignard, M. Hareng, and R. A. Mullen, "Liquid crystal light valve using bulk monocrystalline $Bi_{12}SiO_{20}$ as the photoconductive material," *Appl. Opt.* **21**(20), 3706–3712 (1982).
20. L. Samuelson, H. Wieder, C. R. Guarnieri, J. Chevallier, and A. Onton, "Fast photoconductor liquid-crystal light valve," *Appl. Phys. Lett.* **34,** 450–452 (1979).
21. R. A. Street, "Thermal generation currents in hydrogenated amorphous silicon p-i-n structures," *Appl. Phys. Lett.* **57**(13), 1334–1336 (1990).
22. P. R. Barbier and G. Moddel, "Transient recovery of a-Si:H p-i-n photodiodes," *J. Non-Cryst. Solids* **137&138**(2), 1301–1304 (1991).
23. J. Kanicki and D. Bullock, "Ohmic and quasi-ohmic contacts to hydrogenated amorphous silicon thin films," in *Materials Research Society Symp. Proc.* **70,** 379–386 (1986).
24. B. Drevillon, S. Kumar, and P. Roca i Cabarrocas, "In situ investigation of the optoelectronic properties of transparent conductive oxide/amorphous silicon interfaces," *Appl. Phys. Lett.* **54**(21), 2088–2090 (1989).
25. M. A. Lampert and P. Mark, *Current Injection in Solids,* Academic Press, New York (1970).
26. J. B. Chevrier, P. Cambon, R. C. Chittick, and B. Equer, "Use of n-i-p-i-n a-Si:H structure for bistable optically addressed spatial light modulator," *J. Non-Cryst. Solids* **137,** 1325–1328 (1991).

Pierre R. Barbier carried out his undergraduate work in electrical engineering at Ecole Centrale de Lyon in France. In his summers off he worked at Hewlett-Packard in France, GenRad, Inc., in the United States, and IBM in France. He received the MS degree in 1989 and PhD degree in 1993 in electrical engineering at the University of Colorado at Boulder. His research was in the application of amorphous silicon photosensors to optically addressed spatial light modulators. He is currently employed at the Laboratory for Physical Sciences in College Park, Maryland.

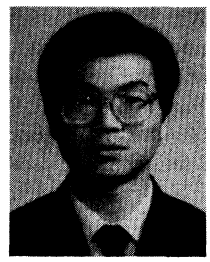

Li Wang received the BS degree in physics in 1984 and MS degree in optics in 1987 from Nankai University in Tianjin, China. He is currently working toward his PhD degree in electrical engineering at the University of Colorado at Boulder. His previous work involved optical thin films and ellipsometry. His current research includes the development of new photosensor materials for optically addressed spatial light modulators and modeling and characterization of the devices.

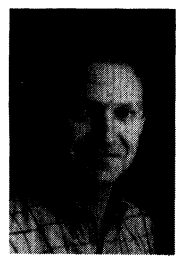

Garret Moddel is an associate professor in the Department of Electrical and Computer Engineering at the University of Colorado at Boulder. He received the BS degree in electrical engineering from Stanford University in 1976 and the MS degree in 1978 and the PhD degree in 1981 in applied physics from Harvard University. From 1981 to 1985 he worked in novel photovoltaic cell designs and processes in a Silicon Valley start-up company before joining the University of Colorado at Boulder. His principal research interests are in amorphous semiconductors and thin-film optoelectronic devices.